Structure and Activity of the Hairpin Ribozyme in Its Natural Junction Conformation: Effect of Metal Ions†

Frank Walter, Alastair I. H. Murchie, James B. Thomson, and David M. J. Lilley*

CRC Nucleic Acid Structure Research Group, Department of Biochemistry, The University, Dundee DD1 4HN, U.K.

Received June 25, 1998; Revised Manuscript Received August 5, 1998

ABSTRACT: The natural form of the hairpin ribozyme consists of a four-way RNA junction of which the single-stranded loop-carrying helices are adjacent arms. The junction can be regarded as providing a framework for constructing the active ribozyme, and the rate of cleavage can be modulated by changing the conformation of the junction. We find that the junction-based form of the hairpin ribozyme is active in magnesium, calcium, or strontium ions, but not in manganese, cadmium, or sodium ions. Using fluorescence resonance energy transfer experiments, we have investigated the global structure of the ribozyme. The basic folding of the construct is based on pairwise helical stacking, so that the two loop-carrying arms are located on opposite stacked helical pairs. In the presence of magnesium, calcium, or strontium ions, the junction of the ribozyme undergoes a rotation into a distorted antiparallel geometry, creating close physical contact between the two loops. Manganese ions induce the same global folding, but no catalytic activity; this change in global conformation is therefore necessary but not sufficient for catalytic activity. Fitting the dependence of the conformation on ionic concentration to a two-state model suggests that cooperative binding of two ions is required to bring about the folding. However, further ion binding is required for cleavage activity. Cobalt hexammine ions also bring about global folding, while spermidine generates a more symmetrical form of the antiparallel structure. Cadmium ions generate a different folded form, interpreted in terms of close loop−loop association while the junction is unfolded. Sodium ions were unable to induce any folding of the ribozyme, which remained slightly parallel. These results are consistent with a folding process induced by the binding of two group IIA metal ions, distributed between the junction and the loop interface.

The hairpin ribozyme is one of a number of small self-cleaving motifs in RNA (reviewed in ref *1*). In the presence of magnesium ions, these ribozymes undergo backbone cleavage via a transesterification reaction whereby the 2′-hydroxyl attacks the adjacent phosphodiester, creating a cyclic 2′,3′-phosphate and a 5′-hydroxyl. The hairpin ribozyme occurs in the negative strand of the satellite RNA of the tobacco ringspot virus (*2*−*4*) and similar plant viruses (*5*). Satellite RNA replicated by a rolling circle becomes processed into monomeric 359 nt RNA molecules by RNA-mediated self-cleavage. The resulting linear species then undergo circularization (*6*), a reaction that is also catalyzed by the hairpin ribozyme (*2*), leading to an equilibrium between cleavage and ligation (*7*).

The viral RNA has extensive secondary structure (Figure 1), but it was shown that the self-cleavage activity was preserved if this was reduced to a form comprising two duplexes, each of which contains formally unpaired loops (the A and B loops), connected by the covalent continuity of one strand (*4*, *8*, *9*). Most studies of this ribozyme have concentrated on this form. Detailed analysis has revealed that the majority of bases (*10*−*12*) and functional groups

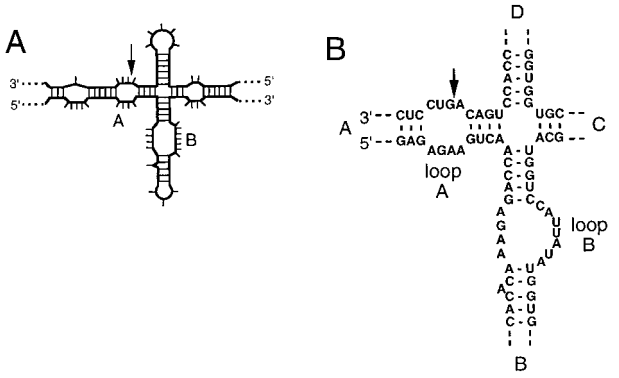

FIGURE 1: Four-way junction of the hairpin ribozyme. (A) Schematic showing the secondary structure of the (−) satellite RNA of the tobacco ringspot virus around the hairpin ribozyme (*4*). Loops A and B are indicated, and the site of ribozyme cleavage is marked with an arrow. (B) The sequence of the hairpin ribozyme in its four-way junction form. The arms are labeled A and B (for the arms containing the A and B loops, respectively) and C and D sequentially.

(*13*−*15*) that are required for activity are located in the loops. It was therefore suspected that physical contact between the loops, with the molecule hinging about the nick, would be required for catalytic activity. This is supported by results from experiments in which the loops have been connected together in a variety of ways with retention of activity; i.e., the ribozyme appears to be active provided that loop−loop

† Supported by grants from the Cancer Research Campaign and the Biotechnology and Biological Sciences Research Council.

* To whom correspondence should be addressed. Telephone: 44-1382 344243. Fax: 44-1382 201063. E-mail: dmjlilley@bad.dundee.ac.uk.

S0006-2960(98)01513-X CCC: $15.00
Published on Web 09/18/1998

interaction can occur (*16*−*21*). Some activity is even possible in trans, when the loop-carrying duplexes are unconnected (*17*, *22*). Chemical cross-linking data support loop−loop interaction (*21*), and very recently, we and others have provided direct physical evidence for the close approach of the loop-bearing duplexes using fluorescence resonance energy transfer (*23*, *24*).

Closer inspection of the local secondary structure around the self-cleavage region shows that the two loop-carrying arms of the conventional hairpin ribozyme constitute two arms of a perfect four-way helical junction [4H junction (*25*)]. We have shown that the ribozyme is active in this form (*23*). In general, four-way RNA junctions are folded by pairwise coaxial stacking under all conditions (*26*, *27*), but the angle subtended between the two resulting helical axes is strongly dependent on conditions. For interaction between the loops of the hairpin ribozyme to be possible, the junction would need to adopt the stacking conformer that places them on different stacks (if the loop-bearing arms were stacked with each other, no amount of rotation could bring them into interaction) and the junction would need to rotate into an antiparallel conformation. We have shown that the structure does indeed adopt the conformer in which the loop-carrying arms are present on different stacked helical pairs (*23*). At very low magnesium ion concentrations, the angle between the axes is approximately 90°, and thus, the loops must be held apart. When the magnesium ion concentration is increased to $\geq 100\ \mu$M, the ribozyme folds into a distorted antiparallel structure characterized by close approach of the A and B loops. It seems highly probable that this conformational transition is a prerequisite for catalytic activity.

We have shown that the activity of the ribozyme in its natural form can be modulated by the conformation of the four-way junction (*23*). The junction provides a framework on which the loops are presented, and it is thus a key conformational component in the formation of the active ribozyme. In previous studies of four-way helical junctions in DNA (*28*, *29*) and RNA (*26*, *27*), a critical role of metal ions has been evident. In this study, we show that the junction form of the ribozyme is functionally folded by group IIA metals, but not by sodium ions. However, we show that the global folding is not by itself sufficient to generate catalytic activity. A study of a number of metal ions with different chemistries leads to the proposal that two ions are generally required for folding the ribozyme, and that these are distributed between the four-way junction and the loop interface in some manner.

MATERIALS AND METHODS

Preparation of the Hairpin Ribozyme and Derived Constructs. DNA and mixed DNA−RNA oligonucleotides were synthesized using phosphoramidite chemistry (*40*). Fluorescently labeled species were prepared as described in ref *41*, with an average efficiency of fluorophore conjugation of 97%. RNA was synthesized using ribonucleotide phosphoramidites with 2′-*tert*-butyldimethylsilyl (TBDMS) protection (*42*, *43*) (Milligen). 6-Fluorescein (PE-ABI) and indocarbocyanine (Cy-3; Glen Research) were coupled to the 5′-termini as phosphoramidites. Oligoribonucleotides were deprotected in a 25% ethanol/ammonia solution at 55 °C for 6 (dye-labeled) or 12 h (unlabeled) and evaporated to dryness. Oligoribonucleotides were redissolved in 0.5 mL of 1 M tetrabutylammonium fluoride (TBAF; Aldrich) in tetrahydrofuran to remove TBDMS groups and agitated at 20 °C in the dark for 16 h prior to desalting by G25 Sephadex (NAP columns; Pharmacia) and ethanol precipitation. Fully deprotected oligonucleotides were purified by gel electrophoresis in 20% polyacrylamide containing 7 M urea; fluorescently labeled species were significantly retarded in the gel system. Bands were excised, and the oligonucleotides were electroeluted into 8 M ammonium acetate and recovered by ethanol precipitation. Fluorescently labeled oligonucleotides were further purified by reversed phase HPLC. Oligonucleotides were dissolved in 100 mM ammonium acetate and applied to a C18 reverse phase column (μ Bondapak, Waters). The RNA was eluted with a linear gradient of acetonitrile; buffer A was 100 mM ammonium acetate and buffer B acetonitrile, with a flow rate of 1 mL/min. The peak fractions were evaporated to dryness, redissolved in water, and then ethanol precipitated. Absorption spectra of fluorescently labeled RNA was recorded on a Cary 1E spectrometer.

Fluorescent hairpin ribozyme species for FRET studies were constructed from two unlabeled strands, one strand labeled with fluorescein and one Cy-3-labeled strand, thus placing the required fluorescein−Cy-3 pair at the ends of chosen arms. The molecules were hybridized by incubating stoichiometric amounts of the four appropriate RNA oligonucleotides in 90 mM Tris-borate (pH 8.3) and 25 mM NaCl for 10 min at 80 °C, followed by slow cooling. The hybridized species were loaded onto a 8% polyacrylamide gel and electrophoresed at 4 °C for 22 h at 150 V. The buffer contained 90 mM Tris-borate (pH 8.3) and 25 mM NaCl and was recirculated at >1 L/h. The fluorescent junctions were visualized by exposure to a standard lamp. The bands were excised, and the RNA was electroeluted into 8 M ammonium acetate and recovered by ethanol precipitation.

Transcription of RNA. RNA was transcribed from synthetic DNA templates using T7 RNA polymerase as described in ref *44* and purified by polyacrylamide gel electrophoresis.

Analysis of Ribozyme Cleavage. Cleavage experiments were carried out under single-turnover conditions (*45*). Ribozyme and 5′-^{32}P-labeled substrate were individually incubated in 50 mM Tris-HCl (pH 7.5) at 90 °C for 2 min, followed by 15 min at 25 °C. Metal salts were added to 10 mM, and incubation was continued for a further 60 min. The reaction was initiated by mixing ribozyme and substrate at 1 μM and 50 nM final concentrations, respectively. The cleavage reactions were stopped at the indicated times, and product formation was analyzed by electrophoresis on sequencing gels containing 7 M urea and autoradiography.

The substrate strand was chemically synthesized, with the sequence (all sequences written 5′ to 3′) UUCGGCCAC-CUGACAGUCCUGUGG. The ribozyme was prepared by transcription, and had the sequence GGCCACAGAGAAGU-CAACCAGAGAAACACACGUUGUGGUAUAUUACCU-GGUACGCCGAAAGGCGUGGUGGCCGAA.

Fluorescence Spectroscopy. Spectroscopy was performed on an SLM-Aminco 8100 fluorimeter operating in the photon counting mode, and spectra were corrected for lamp fluctuations and instrumental variations. Polarization artifacts were

avoided by setting excitation and emission polarizers at 54.74°. Values of E_{FRET} were measured using the $(ratio)_A$ method (*31*, *34*). An extracted acceptor spectrum $F^A(\nu_1,\nu')$ (excitation at $\nu' = 490$ nm, with emission at ν_1) is normalized to a second spectrum $[F(\nu_2,\nu'')]$ from the same sample excited at a wavelength ($\nu'' = 547$ nm) at which only the acceptor is excited, with emission at ν_2. We then obtain the acceptor ratio:

$$(ratio)_A = F^A(\nu_1,\nu')/F(\nu_2,\nu'') = \{E_{FRET}d^+[\epsilon^D(\nu')/\epsilon^A(\nu'')] + [\epsilon^A(\nu')/\epsilon^A(\nu'')]\}[\Phi^A(\nu_1)/\Phi^A(\nu_2)] \quad (1)$$

Superscripts D and A refer to the donor and acceptor, respectively. ϵ^D and ϵ^A are the molar absorption coefficients at the indicated frequency of the donor and acceptor, respectively, and Φ^A is the fluorescent quantum yield of the acceptor. E_{FRET} may be calculated from $(ratio)_A$ since $\epsilon^D(\nu')/\epsilon^A(\nu'')$ and $\epsilon^A(\nu')/\epsilon^A(\nu'')$ are measured from absorption spectra, and $\Phi^A(\nu_1)/\Phi^A(\nu_2)$ is unity when $\nu_1 = \nu_2$.

Fluorescence spectra were recorded at 5 °C in 90 mM Tris-borate (pH 8.3) with the indicated concentrations of salts. Manganese salt solutions were degassed by vacuum followed by passage of argon, and stored and studied under argon. Efficiencies calculated in the presence of hexammine cobalt and spermidine were corrected for quenching. The donor fluorescence intensity was measured as a function of ion concentration, and the ratio of F_0/F_I (where F_0 is the fluorescence intensity in the absence of added ion and F_I is the intensity at a given concentration) plotted as a function of ion concentration (Stern−Volmer plot) was used to correct the E_{FRET} values. The values in the presence of the other ions were uncorrected.

Values of fluorescence anisotropy (r) were determined from measurements of fluorescence intensities using vertical excitation and emission polarizers ($F_{||}$) and vertical excitation and horizontal emission polarizers ($F_\perp$, corrected for detector sensitivity). Fluorescence anisotropy was calculated from

$$r = (F_{||} - F_\perp)/(F_{||} + 2F_\perp) \quad (2)$$

FRET experiments were with performed hairpin species derived from the following oligonucleotides: CCGACCUUCGGCCACCUGACAGUCCUGUGCGG, CCCCACGUCAAGGCGUGGUGGCCGAAGGUCGG, CCGGUGGUAUAUUACCUGGUACGCCUUGACGUGGGG, and CCGCACAGAGAAGUCAACCAGAGAAACACACCGG.

RESULTS

Hairpin Ribozyme in Its Junction Conformation. In the full secondary structure of the negative strand of the tobacco ringspot virus satellite RNA, the hairpin ribozyme is part of a four-way helical junction, in which the A and B loops of the conventional minimized hairpin ribozyme are adjacent arms (Figure 1). In our nomenclature, these arms are named A and B, respectively, and the remaining arms are called C and D, respectively. In all our experiments, we have kept the sequences of arms A, B, and D identical to those of the natural sequence, while arm C has been extended as a perfect duplex for increased stability.

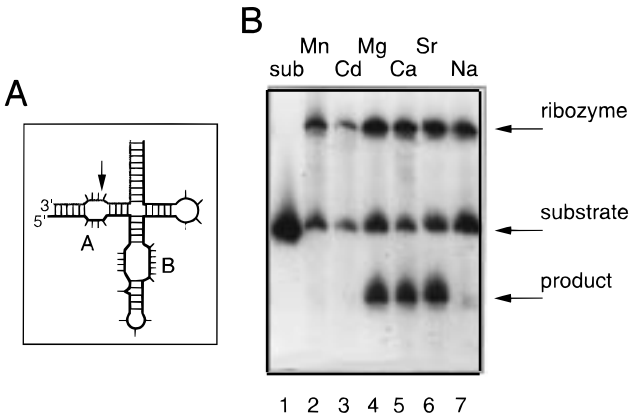

FIGURE 2: Cleavage activity of the junction form of the hairpin ribozyme as a function of metal ions. (A) Scheme showing the ribozyme−substrate construct used in these experiments. The ribozyme (black) comprises a single strand generated by transcription with [α-^{32}P]CTP, forming the B and C arms as hairpin loops. The 5′-^{32}P-labeled substrate (gray) is synthetic. (B) The ribozyme−substrate construct was incubated in 50 mM Tris-HCl (pH 7.5) at 25 °C in the presence of different metal ions each at 10 mM, and the products were analyzed by polyacrylamide gel electrophoresis and autoradiography. The positions corresponding to the migration of the ribozyme strand, full-length substrate, and product are indicated (right). Track 1 contains substrate strand alone. The following metal ions were examined: track 2, Mn^{2+} with a 24 h incubation; track 3, Cd^{2+} with a 24 h incubation; track 4, Mg^{2+} with a 30 min incubation; track 5, Ca^{2+} with a 30 min incubation; track 6, Sr^{2+} with a 30 min incubation; and track 7, Na^+ with a 3 h incubation.

Activity of the Hairpin Ribozyme in Different Metal Ions. We have previously shown that the junction form of the hairpin ribozyme is active in the presence of magnesium ions. The minimized hinged form of the ribozyme has been shown to be active in a variety of divalent metal ions, and we wanted to determine if other ions could activate the junction form. For this purpose, we employed a strategy used previously that avoids the possibility of partial hybridization creating a species equivalent to the hinged form. This approach uses a species comprising just two strands (Figure 2A), a transcribed ribozyme strand to which is hybridized a 5′-^{32}P-labeled synthetic substrate strand. It is difficult to see how this form of the ribozyme could assemble in anything but the complete four-way junction conformation. The reaction was carried out in the presence of 10 mM metal ions under single-turnover conditions at 25 °C, and the products were analyzed by gel electrophoresis (Figure 2B). Inspection of the gel shows that the junction form of the hairpin ribozyme is active in the presence of calcium and strontium ions in addition to the known activity in magnesium ions. By contrast, no activity was detected in the presence of manganese or cadmium ions, or the monovalent sodium ions, even after prolonged incubation.

Fluorescence Resonance Energy Transfer in the Study of Global Structure. We have previously shown that fluorescence resonance energy transfer (FRET) is a powerful method for the study of the global conformation of four-way RNA junctions, including the hairpin ribozyme (*23*, *27*). The six possible relative end-to-end distances (each of which can be studied in both directions) can be compared by this approach, from which the global structure of the molecule

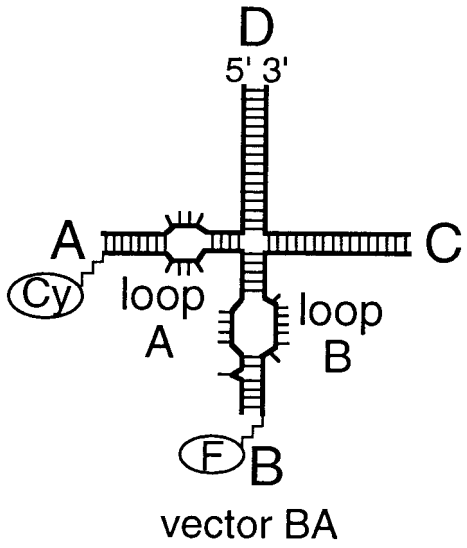

FIGURE 3: Study of the global conformation by fluorescence resonance energy transfer. For the analysis, we compare the six different end-to-end vectors. Each vector can be studied in either direction, though we have shown previously that closely similar results are obtained irrespective of the direction of labeling (*23*). The combinations of the ribozyme with fluorescein and Cy-3 attached to different 5′-termini were synthesized and assembled. The doubly labeled species are named according to the labeled arms, in the order donor−acceptor. The BA vector $B_{(fluorescein)}$-$A_{(Cy-3)}$ is illustrated. Ribozyme cleavage was prevented by replacing the adenine at the cleavage position by deoxyriboadenosine.

may be deduced if the arms have similar lengths. In this method, donor and acceptor fluorophores are attached to the ends of a given pair of helical arms, and the efficiency of energy transfer (E_{FRET}) from the donor to the acceptor is measured. This is inversely related to the sixth power of the distance between the fluorophores (*30*),

$$E_{FRET} = [1 + (R/R_0)^6]^{-1} \quad (3)$$

where R is the distance between the two fluorophores. R_0 is characteristic of the fluorophores used, and is the distance at which E_{FRET} is half-maximal. For a straightforward interpretation of E_{FRET} in terms of distance, we require that one of the fluorophores be mobile. We have measured the anisotropy of the fluorescein attached to the duplex arm as an r of 0.120 in the presence of 90 mM Tris-borate (pH 8.3), indicating that the fluorophore is mobile.

Fluorescein (donor) and cyanine-3 (Cy-3, acceptor) were attached to the 5′-termini of component strands of a junction-based hairpin ribozyme construct (Figure 3). Each helix in the hairpin constructs terminated in a 5′-CC sequence to provide a constant environment for the fluorophores, since we have previously found that this provides a well-behaved environment for FRET measurements in nucleic acids (*31*−*33*). The riboadenine at the A-1 cleavage position was replaced with deoxyriboadenine in all the species to prevent ribozyme-induced cleavage from occurring during the experiments. The efficiency of FRET was measured using the $(ratio)_A$ method of normalization of the acceptor fluorescence (*34*). The fluorescent species are named according to the arms carrying the fluorescent dyes, in the order donor−acceptor; e.g., the species BA has fluorescein attached to the end of the B arm and Cy-3 attached to the end of the A arm.

Conformation of the Hairpin Ribozyme in the Presence of Calcium Ions. The measured FRET efficiencies for the six end-to-end vectors for the hairpin ribozyme are compared in Figure 4. In the absence of added metal ions, the six values of E_{FRET} are all low (Figure 4A), indicating a relatively extended structure. The efficiencies for the BD and CA vectors are approximately twice those of the remaining vectors, consistent with a structure based on the coaxial stacking of A on D and B on C arms, with a slight rotation into a parallel structure. On addition of calcium ions at a low concentration, the pattern changes to one in which the E_{FRET} values for vectors DA and BC are smaller than those for the remaining four vectors (Figure 4B), consistent with a 90° crossed structure. On addition of calcium ions at higher concentrations ($\geq 100\ \mu M$), the pattern of E_{FRET} values changes considerably (Figure 4C). While the values for vectors DA, AC, and BC remain small (<0.08), the remaining three vectors exhibit considerably enhanced efficiency of energy transfer in the order AB > DC > DB. This pattern is closely similar to that observed in the presence of magnesium ions (*23*), which has been interpreted in terms of an antiparallel junction (based on pairwise A on D and B on C coaxial stacking) that is distorted by the close approach of the A and B arms. This suggests that both calcium and magnesium can induce the structural transition that involves the interaction between the A and B loops.

A finer titration of the calcium-induced folding of the hairpin ribozyme followed by the change in E_{FRET} of the BA vector is shown in Figure 4D. We have previously shown that similar data can be fitted to a simple two-state model in which the FRET-observable transition between conformations is induced by the binding of n ions with an apparent association constant K_A. The proportion of junction in the antiparallel form (α) will be given by

$$\alpha = K_A[Mg^{2+}]^n/(1 + K_A[Mg^{2+}]^n) \quad (4)$$

Using this model, we obtained an excellent fit to the data for the shortening of the BA vector, where $n = 2.01$. This is consistent with a transition induced by the binding of two calcium ions, i.e., the same stoichiometry as that observed for magnesium ions (*23*). The apparent association constant calculated for two-ion-induced folding was $2.15 \times 10^9\ M^{-2}$. The analysis was repeated for the CD vector, with calculated values for n of 1.95 and for K_A of $9.2 \times 10^8\ M^{-2}$. In corresponding experiments with magnesium ions (data not shown), we obtained values for n of 2.15 and 2.10 for the BA and AB vectors, respectively, with corresponding apparent association constants of 1.89×10^9 and $1.76 \times 10^9\ M^{-2}$ calculated for a two-ion-induced process.

Conformation of the Hairpin Ribozyme in the Presence of Strontium Ions. Calcium and magnesium ions are both group IIA metal ions, with similar chemistries. We therefore examined the next member of the group, strontium, which also results in cleavage activity of the junction form of the ribozyme (Figure 2). This ion induced apparently identical folding in the hairpin ribozyme (Figure 5), with the same close approach of the A and B arms. Fine titration of the BA vector indicated two-ion-induced folding once again ($n = 1.98$), with a K_A of $2.52 \times 10^9\ M^{-2}$. Thus, the folding properties of the three group IIA metal ions are closely similar.

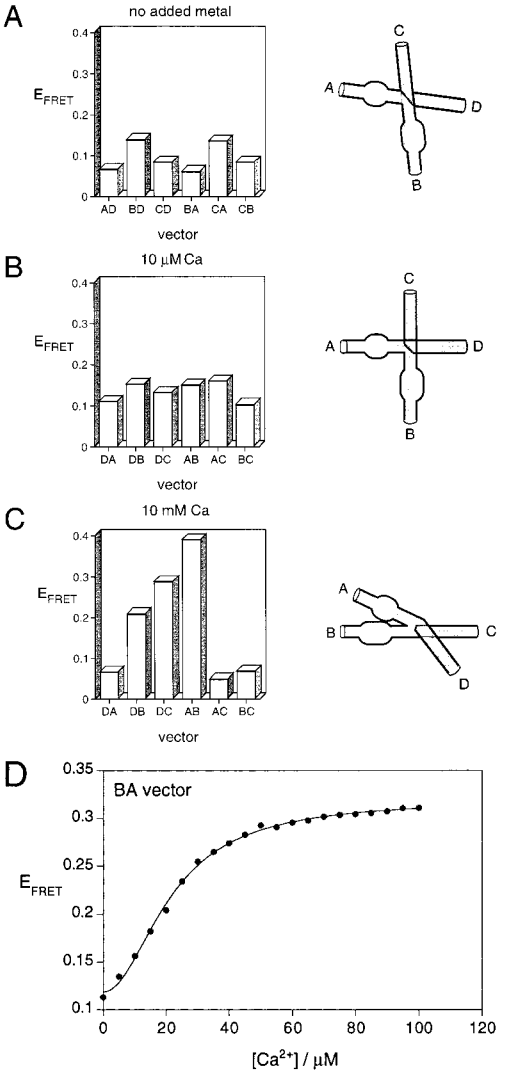

FIGURE 4: Analysis of the global conformation of the hairpin ribozyme in the presence of calcium ions. The data are presented as histograms of measured FRET efficiencies for six end-to-end vectors. In the case of panel A, these are reversed with respect to the remaining set. (A) Global conformation in the absence of added metal ions. The FRET analysis was carried out in 90 mM Tris-borate (pH 8.3) and 0.1 mM EDTA. The low values of E_{FRET} indicate an extended structure. The higher values for the BD and CA vectors indicate a slightly parallel form of a structure based on A on D and B on C coaxial stacking (indicated on the right). (B) Comparison of E_{FRET} values for the alternative set of six end-to-end vectors in the presence of 10 μM calcium ions. All six values remain relatively low, indicative of an extended structure, but the slightly lower values for DA and BC are consistent with a calcium-induced rotation into a 90° crossed structure based on A on D and B on C stacking (indicated on the right). (C) E_{FRET} values in the presence of 10 mM Ca^{2+} ions for the same set of end-to-end vectors used in panel B. In the presence of the higher calcium ion concentration, the structure has clearly changed, with efficiencies in the order AB > DC > DB. This is consistent with the formation of a structure in which the end-to-end vector for helices A and B is the shortest such distance (shown right). (D) Folding of the hairpin ribozyme over the range of 0−100 μM Ca^{2+} ions followed by the change of E_{FRET} for the shortest vector BA. The experimental data (●) were fitted by regression to a simple binding model where the binding of *n* ions to the RNA induces a global structural change between two conformations. The line shows the best fit to this model.

Conformation of the Hairpin Ribozyme in the Presence of Manganese Ions. In many respects, the chemistries of manganese and magnesium ions are similar, since they differ only in a spherically symmetrical half-filled d shell in the former ion (i.e., $4s^2 3d^5$ configuration). Yet manganese ions are unable to generate catalytic activity in the hairpin ribozyme (Figure 2). Analysis of FRET efficiencies for the six end-to-end vectors (Figure 6A) shows that despite the lack of activation of ribozyme activity, apparently identical global folding is induced. Finer titration of the BA vector (Figure 6B) shows that the folding appears to be induced by the binding of two manganese ions ($n = 1.94$) with a K_A of 4.69×10^9 M^{-2}. Thus, the failure to achieve cleavage in the ribozyme does not appear to reflect a defect in the folding of the global structure, and close approach of the A and B loops occurs as before.

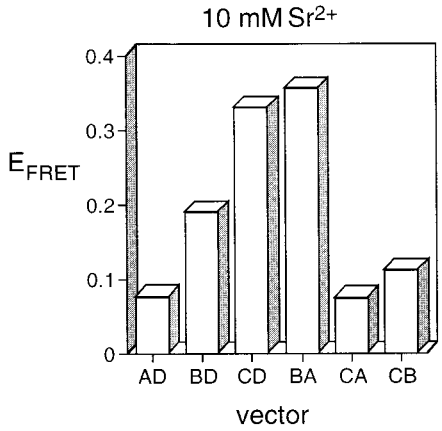

FIGURE 5: Analysis of the global conformation of the hairpin ribozyme in the presence of strontium ions. Comparison of E_{FRET} values for the six end-to-end vectors in the presence of 10 mM Sr^{2+} ions. The pattern of efficiencies is closely similar to that observed in the presence of calcium ions (Figure 4C), indicating that the same distorted antiparallel structure is formed.

Conformation of the Hairpin Ribozyme in the Presence of Hexammine Cobalt(III) Ions. Several groups have shown that the hinged form of the hairpin ribozyme is active in the presence of hexammine cobalt(III) ions (*35*−*37*). We therefore sought to examine the global folding in the presence of this complex ion. The results show (Figure 7A) that the global structure is closely similar to that induced by the other ions, with the same BA > CD > BD pattern of efficiencies. Hexammine cobalt(III) ions are significantly more efficient in promoting the folding of the hairpin ribozyme than the divalent ions considered above. Fine titration of the BA vector (Figure 7B) shows that the apparent association constant has risen to 1.73×10^{13} M^{-2}. The value for *n* of 1.75 suggests that two ions are required, although there is probably some reduction in the cooperativity of binding.

Folding of the Hairpin Ribozyme Induced by Spermidine. In addition to metal ions, polyamines are also efficient in promoting structural transitions in nucleic acids. We have therefore examined the global conformation of the hairpin ribozyme as a function of spermidine concentration (Figure 7C). In broad terms, the pattern of FRET efficiencies is similar to those seen with the metal ions, although the eventual pattern in the presence of 5 mM spermidine is rather more symmetrical than the previous ones, such that E_{FRET} values for BA and CD are very similar, as are the values for BD and CA. However, fine titration of the BA vector (Figure 7D) shows that the characteristics of the spermidine-induced folding are rather different. Folding appears to be

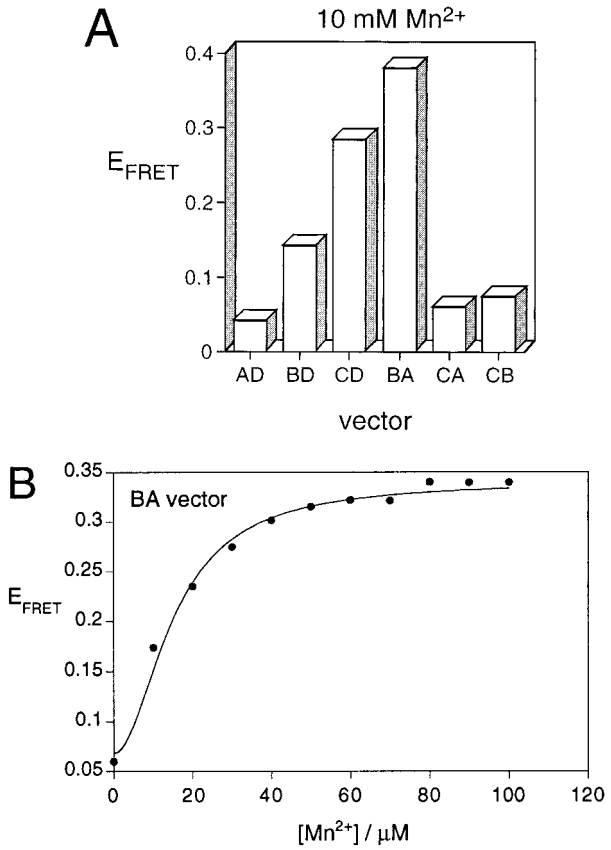

FIGURE 6: Analysis of the global conformation of the hairpin ribozyme in the presence of manganese ions. (A) Comparison of E_{FRET} values for the six end-to-end vectors in the presence of 10 mM Mn^{2+} ions. The pattern of efficiencies is closely similar to those observed in the presence of calcium and strontium ions (Figures 4C and 5, respectively), indicating that a globally similar distorted antiparallel structure is formed. (B) Folding of the hairpin ribozyme over the range of 0−100 μM Mn^{2+} ions followed by the change of E_{FRET} for the shortest vector BA. The experimental data (●) were fitted by regression to the simple two-state binding model as before. The line show the best fit to this model.

promoted by the binding of a single spermidine molecule ($n = 1.11$) and occurs at a relatively high concentration of the polyamine (in the millimolar range, corresponding to a K_A of 9266 M^{-1} calculated for single-ion-induced folding).

A Different Global Conformation of the Hairpin Ribozyme in the Presence of Cadmium Ions. Cadmium is a group IIB metal ($5s^2 4d^{10}$), with chemistry very different from that of the group IIA metal ions studied above. As we showed above, the hairpin ribozyme in its junction form is not active in the presence of cadmium ions. We examined the global conformation of the hairpin ribozyme as a function of cadmium ion concentration (Figure 8A) and obtained a pattern of FRET efficiencies that is different from all those found previously. At concentrations of ≥1 mM, five of the six end-to-end vectors exhibit E_{FRET} values of 0.2−0.3, but the BA vector is quite different from the rest with a value of 0.5−0.6. This indicates that all the end-to-end distances are relatively long except for B−A and suggests a relatively extended structure for the junction except for a close approach of the A and B arms that is presumably driven by cadmium-induced association of the A and B loops. Titration of the BA vector (Figure 8B) showed that the shortening of this distance is fitted to a cadmium binding-induced folding corresponding to the binding of a single cadmium ion ($n = 1.04$) with a K_A of 1405 M^{-1} (calculated for single-ion-induced folding).

Conformation of the Hairpin Ribozyme in the Presence of Sodium Ions. The junction form of the hairpin ribozyme is inactive in the presence of sodium ions (Figure 2), and group IA metal ions have been shown to inhibit the cleavage reaction of the hinged form of the ribozyme (*38*). The patterns of FRET efficiency for the six vectors change very little as a function of sodium ion concentration (Figure 9). Even in the presence of 100 mM sodium ion and 0.1 mM EDTA, none of the E_{FRET} values rises higher than 0.20, indicating that the molecule remains in an extended conformation. Vectors DB and AC have slightly larger E_{FRET} values than the remaining four vectors. This pattern is closely similar to that in the absence of added metal ions (Figure 4), consistent with a small rotation of the stacked structure in the parallel direction. Clearly, the monovalent ion is quite unable to induce the association of the A and B loops.

DISCUSSION

The global structure of the hairpin ribozyme in its natural form as a four-way junction undergoes a number of ion-induced changes. Like that in other four-way junctions in RNA (*26*, *27*), coaxial stacking of helices is preserved under all conditions, with the loop-carrying arms (A and B) on different stacked pairs. In the absence of added ions, the overall conformation is slightly parallel, with the loops held well apart as a consequence. With the addition of a low concentration of group IIA metal ions (typically, 10 μM), the helices rotate such that the two axes become perpendicular. Increasing the ionic concentration to ≥100 μM causes the helices to rotate into a distorted antiparallel structure, with a close approach of the loop-carrying arms. While we have previously observed this behavior in response to the addition of magnesium ions (*23*), we now show that this is true also for calcium and strontium ions, and is probably general for the group IIA metal ions. By contrast, sodium ions are totally unable to promote the formation of the antiparallel structure, and the structure remains slightly parallel even at concentrations as high as 100 mM.

Magnesium, calcium, and strontium ions also promote the cleavage reaction of the junction form of the hairpin ribozyme, while no activity was seen in the presence of sodium ions. Interestingly, however, while manganese ions appear to induce the formation of the same globally folded structure as that found in the presence of the group IIA metal ions, the ribozyme is inactive in the presence of this ion. This indicates that the global folding of the ribozyme is not of itself sufficient to generate catalytic activity. A further indication of this is given by the different concentration ranges of the ions that are required for global folding and for cleavage. While the folding occurs in the micromolar region for the hairpin form of the ribozyme, cleavage requires millimolar concentrations of these ions. This indicates that further ion binding is required, which is not accompanied by changes in the global folding.

The change in the conformation of the junction-based ribozyme induced by the group IIA metal ions can be analyzed in terms of a simple two-state folding process. This model assumes that a number (n) of ions are required to bind

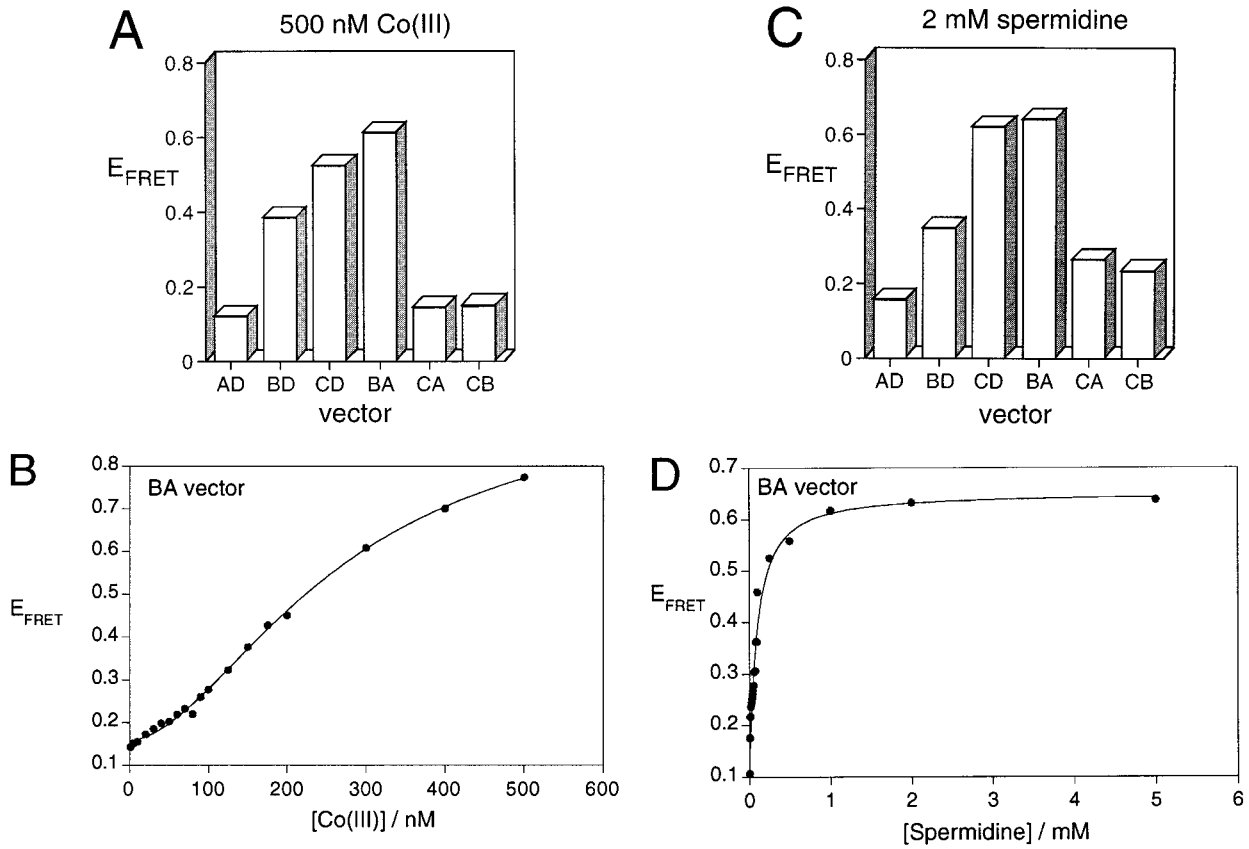

FIGURE 7: Analysis of the global conformation of the hairpin ribozyme in the presence of cobalt hexammine ions and spermidine. (A) Comparison of E_{FRET} values for the six end-to-end vectors in the presence of 500 nM $Co(NH_3)_6^{2+}$ ions. The pattern of efficiencies is closely similar to those observed in the presence of calcium, strontium, and manganese ions (Figures 4C, 5, and 6, respectively), indicating that a globally similar distorted antiparallel structure is formed. $Co(NH_3)_6^{2+}$ ions quench the fluorescence of fluorescein very efficiently, and this requires correction. This may result in an overall elevation of the magnitudes of the efficiencies. (B) Folding of the hairpin ribozyme over the range of 0−500 nM $Co(NH_3)_6^{2+}$ ions followed by the change of E_{FRET} for the shortest vector BA. Clearly, the titration is incomplete over this range, but fluorescein quenching prevents higher $Co(NH_3)_6^{2+}$ ion concentrations from being possible. The experimental data (●) were fitted by regression to the simple two-state binding model. The line shows the best fit to this model. (C) Comparison of E_{FRET} values for the six end-to-end vectors in the presence of 2 mM spermidine. The pattern of efficiencies is related to those observed in the presence of calcium, strontium, and manganese ions (Figures 4C, 5, and 6, respectively), but is more symmetrical. As with $Co(NH_3)_6^{2+}$ ion, fluorescein quenching required correction of the data, elevating the absolute E_{FRET} values. (D) Folding of the hairpin ribozyme over the range of 0−5 mM spermidine followed by the change of E_{FRET} for the shortest vector BA. The experimental data (●) were fitted by regression to the simple two-state binding model. The line show the best fit to this model.

before the FRET-observed change occurs (corresponding to binding with full cooperativity), and fitting of the experimental data gives a consistent value of 2 ions for the group IIA metals and manganese. This corresponds to apparent association constants of close to 2×10^9 M^{-2} for the group IIA metal ions. Clearly, more complex binding models cannot be excluded, though these would be very unlikely to give better fits to the experimental data. Strictly speaking, the value of *n* that emerges from the fitting is a Hill coefficient; however, the values very close to 2 that emerge for both short vectors and a number of different metal ions strongly suggest that the folding is induced by the binding of 2 ions. We have found that when we study the folding of the four-way junction of the hairpin ribozyme in isolation from the loops, we consistently obtain values of for *n* of 1, with a considerably lower binding affinity (A. I. H. Murchie, F. Walter, and D. M. J. Lilley, submitted for publication). It therefore seems probable that two ions are involved in the folding of the complete ribozyme, distributed between the junction and the loops, and cooperative binding of these ions markedly lowers the concentration required to induce folding.

In a number of respects, the properties of the junction-based ribozyme parallel those of the hinged form. The hinged ribozyme was found to be active in magnesium, calcium, and strontium ions, but no cleavage could be observed in the presence of manganese, cadmium, or sodium ions (*38*). In a recent study, Burke and co-workers (*24*) have used a FRET-based assay to study the rate of folding of the hinged form of the ribozyme. They find that association of the loop-carrying arms is promoted by magnesium, calcium, strontium, manganese, and cobalt hexammine ions, but not by monovalent ions. This is clearly very similar to the situation that we observe with the junction form of the ribozyme. However, the concentration of the group IIA metals required for optimal folding rates of the hinged form were in the millimolar range, consistent with a lack of cooperativity of ion binding in this form.

Three recent studies have found that the hairpin ribozyme is active in the presence of cobalt hexammine ions (*35*−*37*), and we show here that the junction form of the ribozyme is folded by very low concentrations of the ion, corresponding to an apparent association constant of close to 2×10^{13} M^{-2}. Cobalt hexammine is also highly efficient in stabilizing

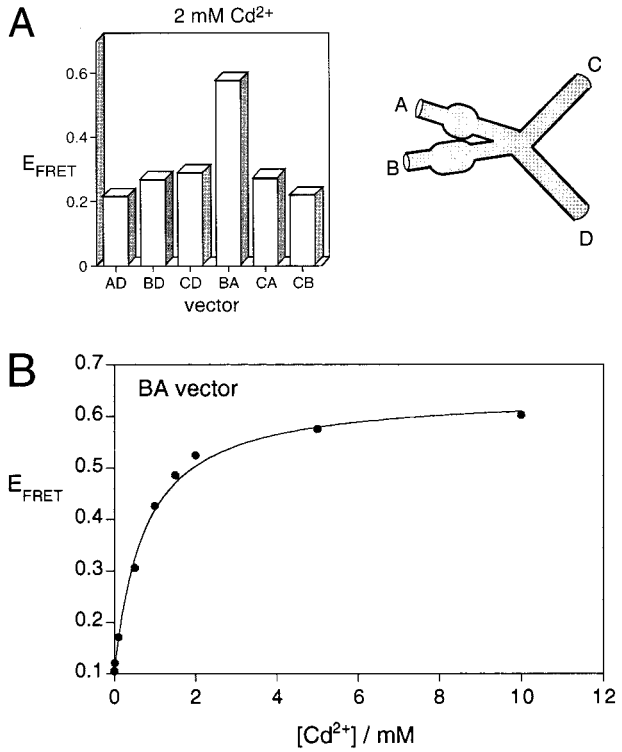

FIGURE 8: Analysis of the global conformation of the hairpin ribozyme in the presence of cadmium ions. (A) Comparison of E_{FRET} values for the six end-to-end vectors in the presence of 2 mM Cd^{2+} ions. The pattern is quite different from those found previously, with a single vector (BA) showing efficient energy transfer. The E_{FRET} data are interpreted in terms of the model for the global folding shown on the right. (B) Folding of the hairpin ribozyme over the range of 0−10 mM Cd^{2+} ions followed by the change of E_{FRET} for the short vector BA. The experimental data (●) were fitted by regression to the simple two-state binding model. The line shows the best fit to this model.

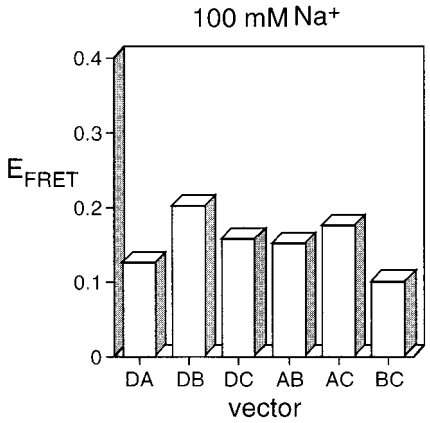

FIGURE 9: Analysis of the global conformation of the hairpin ribozyme in the presence of sodium ions. Comparison of E_{FRET} values for the six end-to-end vectors in the presence of 100 mM Na^+ ions. The pattern of efficiencies is similar to that observed in the absence of added metal ions (Figure 4A), consistent with the formation of a slightly antiparallel structure based on A on D and B on C coaxial stacking.

the folded conformation of DNA junctions (*28*), and the formation of left-handed Z-DNA by alternating $d(CpG)_n$ sequences (*39*). The pattern of FRET efficiencies is closely similar to that generated by the group IIA metals, indicating that inner-sphere complex formation is not required, since the exchange rate of the ammine ligands is extremely slow, but the value for *n* of 1.75 emerging from the titration data suggests that the high affinity might slightly reduce the cooperativity of ion binding. We have also observed that the junction form of the hairpin ribozyme can be folded by spermidine. However, the folding is orders of magnitude less efficient, requiring millimolar concentrations of the polyamine (compared to the sub-micromolar concentration range for cobalt hexammine), and fitting indicates that folding is induced by the binding of a single spermidine molecule. The pattern of FRET efficiencies indicates a more symmetrical global structure for the ribozyme, suggesting that the binding of a single spermidine molecule is unable to induce folding into the same global structure as that generated by the group IIA metal ions. In fact, the pattern of relative efficiencies for the six end-to-end vectors is similar to that found for the hairpin junction in the absence of the loops (F. Walter, A. I. H. Murchie, and D. M. J. Lilley, submitted for publication), which could indicate that the spermidine is more closely associated with the four-way junction of the ribozyme. The folding induced by cadmium ions may represent the inverse of this. The pattern of FRET efficiencies is quite different from that found in the presence of all the other metal ions, where only the BA vector is significantly shortened on folding. This is consistent with a folded structure of the ribozyme in which cadmium ions induce close loop−loop interaction, but the junction is unfolded to give an extended global structure, probably at the expense of coaxial helical stacking.

Taken together, these results are consistent with a model in which the group IIA metal ions fold the hairpin ribozyme in its natural junction form by binding to the junction and to the loops, and to an extent, these binding events may be differentiated using different ions. Clearly, the conformation of the junction is important to the activity of the ribozyme; we have previously shown that sequence changes that alter the population of stacking conformers at the junction have a significant effect on the rate of the cleavage reaction (*23*). Yet the lack of activity of the ribozyme in the presence of manganese ions, which apparently induce a completely normal global folding, shows that while the formation of this structure is necessary for activity, it is not sufficient. The millimolar concentration of magnesium ions required for efficient cleavage rates indicates an additional role for bound ions. Experiments showing that the substitutionally inert cobalt hexammine ions can promote ribozyme cleavage (*35*−*37*) do not support a direct role for bound metal ion, providing either general base catalysis or electrophilic catalysis as a Lewis acid. It is therefore likely that there are additional structural roles for metal ions which have less impact on the global structure, and which are consequently not observed in the FRET experiments. Ultimately, we expect that these ions generate the correct local RNA conformation in the loop A−B interface to facilitate the trajectory into the in-line transition state for the S_N2 cleavage reaction. But fully understanding the further structural role-(s) of these metal ions remains a challenge.

ACKNOWLEDGMENT

We thank Drs. Bob Clegg, Gurminder Bassi, and Richard Grainger for valuable discussions and Audrey Gough for technical assistance.

REFERENCES

1. Eckstein, F., and Lilley, D. M. J., Eds. (1996) RNA Catalysis, *Nucleic Acids and Molecular Biology*, Vol. 10, Springer-Verlag, Berlin.
2. Buzayan, J. M., Gerlach, W. L., and Bruening, G. (1986) *Nature 323*, 349−353.
3. Feldstein, P. A., Buzayan, J. M., and Bruening, G. (1989) *Gene 82*, 53−61.
4. Hampel, A., and Tritz, R. (1989) *Biochemistry 28*, 4929−4933.
5. DeYoung, M. B., Siwkowski, A. M., Lian, Y., and Hampel, A. (1995) *Biochemistry 34*, 15785−15791.
6. van Tol, H., Buzayan, J. M., and Bruening, G. (1991) *J. Virol. 280*, 23−30.
7. Hegg, L. A., and Fedor, M. J. (1995) *Biochemistry 34*, 15813−15828.
8. Hampel, A., Tritz, R., Hicks, M., and Cruz, P. (1990) *Nucleic Acids Res. 18*, 299−304.
9. Chowrira, B. M., Berzal-Herranz, A., and Burke, J. M. (1991) *Nature 354*, 320−322.
10. Berzal-Herranz, A., Simpson, J., Chowrira, B. M., Butcher, S. E., and Burke, J. M. (1993) *EMBO. J. 12*, 2567−2574.
11. Anderson, P., Monforte, J., Tritz, R., Nesbitt, S., Hearst, J., and Hampel, A. (1994) *Nucleic Acids Res. 22*, 1096−1100.
12. Siwkowski, A., Shippy, R., and Hampel, A. (1997) *Biochemistry 36*, 3930−3940.
13. Chowrira, B. M., Berzal-Herranz, A., Keller, C. F., and Burke, J. M. (1993) *J. Biol. Chem. 268*, 19458−19462.
14. Grasby, J. A., Mersmann, K., Singh, M., and Gait, M. J. (1995) *Biochemistry 34*, 4068−4076.
15. Schmidt, S., Beigelman, L., Karpeisky, A., Usman, N., Sorensen, U. S., and Gait, M. J. (1996) *Nucleic Acids Res. 24*, 573−581.
16. Komatsu, Y., Koizumi, M., Nakamura, H., and Ohtsuka, E. (1994) *J. Am. Chem. Soc. 116*, 3692−3696.
17. Butcher, S. E., Heckman, J. E., and Burke, J. M. (1995) *J. Biol. Chem. 270*, 29648−29651.
18. Komatsu, Y., Kanzaki, I., and Ohtsuka, E. (1996) *Biochemistry 35*, 9815−9820.
19. Komatsu, Y., Kanzaki, I., Shirai, M., and Ohtsuka, E. (1997) *Biochemistry 36*, 9935−9940.
20. Komatsu, Y., Shirai, M., Yamashita, S., and Ohtsuka, E. (1997) *Bioorg. Med. Chem. 5*, 1063−1069.
21. Earnshaw, D. J., Masquida, B., Müller, S., Sigurdsson, S. T., Eckstein, F., Westhof, E., and Gait, M. J. (1997) *J. Mol. Biol. 274*, 197−212.
22. Shin, C., Choi, J. N., Sang, S. I., Song, J. T., Ahn, J. H., Lee, J. S., and Choi, Y. D. (1996) *Nucleic Acids Res. 24*, 2685−2689.
23. Murchie, A. I. H., Thomson, J. B., Walter, F., and Lilley, D. M. J. (1998) *Mol. Cell 1*, 873−881.
24. Walter, N. G., Hampel, K. J., Brown, K. M., and Burke, J. M. (1998) *EMBO J. 17*, 2378−2391.
25. Lilley, D. M. J., Clegg, R. M., Diekmann, S., Seeman, N. C., von Kitzing, E., and Hagerman, P. (1995) *Eur. J. Biochem. 230*, 1−2.
26. Duckett, D. R., Murchie, A. I. H., and Lilley, D. M. J. (1995) *Cell 83*, 1027−1036.
27. Walter, F., Murchie, A. I. H., Duckett, D. R., and Lilley, D. M. J. (1998) *RNA 4*, 719−728.
28. Duckett, D. R., Murchie, A. I. H., and Lilley, D. M. J. (1990) *EMBO J. 9*, 583−590.
29. Møllegaard, N. E., Murchie, A. I. H., Lilley, D. M. J., and Nielsen, P. E. (1994) *EMBO J. 13*, 1508−1513.
30. Förster, T. (1948) *Ann. Phys. 2*, 55−75.
31. Murchie, A. I. H., Clegg, R. M., von Kitzing, E., Duckett, D. R., Diekmann, S., and Lilley, D. M. J. (1989) *Nature 341*, 763−766.
32. Clegg, R. M., Murchie, A. I. H., Zechel, A., Carlberg, C., Diekmann, S., and Lilley, D. M. J. (1992) *Biochemistry 31*, 4846−4856.
33. Clegg, R. M., Murchie, A. I. H., Zechel, A., and Lilley, D. M. J. (1993) *Proc. Natl. Acad. Sci. U.S.A. 90*, 2994−2998.
34. Clegg, R. M. (1992) *Methods Enzymol. 211*, 353−388.
35. Hampel, A., and Cowan, J. A. (1997) *Chem. Biol. 4*, 513−517.
36. Nesbitt, S., Hegg, L. A., and Fedor, M. J. (1997) *Chem. Biol. 4*, 619−630.
37. Young, K. J., Gill, F., and Grasby, J. A. (1997) *Nucleic Acids Res. 25*, 3760−3766.
38. Chowrira, B. M., Berzal-Herranz, A., and Burke, J. M. (1993) *Biochemistry 32*, 1088−1095.
39. Gessner, R. V., Quigley, G. J., Wang, A. H.-J., van der Marel, G., van Boom, J., and Rich, A. (1985) *Biochemistry 24*, 237−240.
40. Beaucage, S. L., and Caruthers, M. H. (1981) *Tetrahedron Lett. 22*, 1859−1862.
41. Bassi, G. S., Murchie, A. I. H., Walter, F., Clegg, R. M., and Lilley, D. M. J. (1997) *EMBO J. 16*, 7481−7489.
42. Hakimelahi, G. H., Proba, Z. A., and Ogilvie, K. K. (1981) *Tetrahedron Lett. 22*, 5243−5246.
43. Perreault, J.-P., Wu, T., Cousineau, B., Ogilvie, K. K., and Cedergren, R. (1990) *Nature 344*, 565−567.
44. Milligan, J. F., Groebe, D. R., Witherall, G. W., and Uhlenbeck, O. C. (1987) *Nucleic Acids Res. 15*, 8783−8798.
45. Thomson, J. B., Sigurdsson, S. T., Zeuch, A., and Eckstein, F. (1996) *Nucleic Acids Res. 24*, 4401−4406.

BI981513+